Femtosecond Near-Infrared Laser Desorption of Multilayer Benzene on Pt{111}: A Molecular Newton's Cradle?†

Heike Arnolds, Christian Rehbein, Gareth Roberts, Robert J. Levis,*,‡ and David A. King*

Department of Chemistry, Cambridge University, Lensfield Road, Cambridge, CB2 1EW, U.K.

Received: October 15, 1999; In Final Form: February 11, 2000

Velocity distributions resulting from the intense, near-IR laser desorption of multilayers of benzene adsorbed on Pt{111} are reported as a function of laser intensity, which was varied by changing fluence and pulse width. The velocity distributions as a function of intensity show characteristics of both thermally and electronically induced desorption. Changing the pulse width from the subpicosecond to the subnanosecond regime only results in a small quantitative change in the velocity distributions, suggesting a similar desorption mechanism for laser pulse duration spanning 3 orders of magnitude. Possible mechanisms are discussed and a new mechanism is proposed in which the process is initiated by a thermally assisted DIET excitation in the chemisorbed layer, and followed by energy transfer from the Pt−benzene interface to the outermost benzene layers via a molecular Newton's cradle mechanism.

I. Introduction

Recently, the intense near-infrared laser desorption of intact benzene molecules has been reported.[1] Three distinct translational distributions were observed and were labeled the hyperthermal or prompt, thermal, and subthermal features according to their respective kinetic energies. The desorbing material that makes up the prompt feature had a translational temperature of up to a few thousand degrees kelvin and originated mainly in the outermost layers of the film for coverage up to 20 ML (ML = monolayer) of benzene. Such a desorption process would be expected if the multilayer species was strongly absorbing at the excitation wavelength as in the matrix-assisted laser desorption (MALD) experiment.[2] However, the benzene multilayer is transparent to excitation at 800 nm. The desorption mechanism of such transparent multilayers adsorbed on metallic surfaces remains essentially unknown and has only been investigated for films of submicrometer thickness.[3] One hypothesis is that the desorption process is due to the femtosecond duration of the laser pulse. The ultrashort pulse results in laser intensities that are several orders of magnitude larger than the intensities employed in nanosecond experiments.

To begin to elucidate the mechanism of desorption, we investigate here the velocity distributions of desorbed benzene over a wide range of intensities by varying both fluence and pulse width of the exciting laser beam. Our observations provide further evidence for a unique desorption phenomenon for transparent multilayer systems on transition metal surfaces.

There are at least three different standard models that may be proposed to describe the intense laser desorption of multilayers: the thermal, impulsive, and electronic.

In a purely thermal mechanism one expects a Maxwell−Boltzmann distribution of desorbing molecules corresponding to the temperature of the substrate at the time of desorption. However, collisions in the gas phase after desorption may serve to alter the pure thermal distribution to one having a stream velocity.[4] The high heating rates achievable (10^{10} K/s) favor desorption of intact molecules over reaction.[5]

In the impulsive mechanism a velocity distribution corresponding to a modified Maxwell−Boltzmann distribution having a stream velocity offset is expected. An example of impulsive[6] desorption is given by the photochemical ejection of methyl bromide from a LiF{0001} surface.[7] It is important to note that in the case of impulsive desorption the adsorbate normally strongly absorbs the incident radiation because desorption is mediated by the repulsive portion of the potential energy surface.

In the case of electron-induced desorption a range of desorption profiles may be observed. In the case of desorption induced by electronic transitions (DIET) the desorbate distribution is nominally Maxwell−Boltzmann[8] and the cross section for desorption increases linearly with laser intensity. This is because the desorption process involves a single electronic excitation. The velocity of the desorbate does not increase appreciably as the laser intensity is increased but has been observed to increase as the wavelength of the incident laser is decreased.[9] In the case of desorption induced by multiple electronic transitions (DIMET) the intensity of the desorbate signal is known to increase nonlinearly with laser intensity.[10] This is thought to be a signature of the multielectron nature of the adsorbate excitation prior to desorption. In the case of DIMET there is a correlation between the desorbate kinetic energy and the incident laser intensity.[11]

A nonlinear increase of yield with fluence is also observed in the case of MALD. In the case of absorbing condensed phase systems, such as MALD, there is no strong dependence of the gas phase velocity distribution on the incident pulse energy,[12] but the amount of desorbing material has been measured to scale as the sixth power of the incident laser intensity.[13] However, since the ions created during the desorption process determine the velocity distribution, the sixth-order dependence does not necessarily imply an electronic desorption mechanism.

There are three time scales that are important for laser desorption: the time scales for electronic and phonon excitation and the time scale for desorption of the adsorbate. The initial

* Corresponding authors.

† Part of the special issue "Gabor Somorjai Festschrift".

‡ Camille Dreyfus Teacher Scholar and Sloan Fellow. Permanent address: Department of Chemistry, Wayne State University, Detroit, MI.

10.1021/jp993688e CCC: $19.00
Published on Web 03/09/2000

excitation in DIET and DIMET occurs on the electronic time scale (electron mediated),[14] while in conventional nanosecond laser desorption the excitation occurs on the nuclear time scale (phonon mediated).[15] In either mechanism, desorption occurs on the time scale set by the amount of excitation and the mass of the adsorbate. Altering the laser pulse duration may cause an observable change from electronic to phonon excitation. This is because the shortest duration laser pulse initially produces a nonequilibrium partitioning between electron and phonon heat baths. At short times (up to a few hundred femtoseconds), the electronic modes are primarily excited,[16] while equilibration with the lattice occurs over a picosecond time scale. For longer duration laser pulses the electron and lattice temperatures remain in equilibrium and the two-photon photoemission can be used to determine the lattice temperature.[17] To determine whether electronic or phonon mechanisms dominate in the desorption mechanism we probed the time-of-arrival distributions for multilayers of benzene at different laser pulse widths.

The C_6H_6/Pt{111} system has been well characterized using conventional surface analytical methods.[18−21] Benzene forms a well-defined series of binding states on the Pt{111} surface when adsorbed at 120 K. Molecules first adsorb in a chemisorbed layer that desorbs between 200 and 500 K. A series of three physisorption states are formed sequentially at higher coverage.[22] As described previously, in the α_1 state the molecules are initially oriented parallel to the surface. Upon further exposure, α_1 molecules rearrange into a more crowded, amorphous layer at high average tilt angle (the α_2 state). This state is metastable and converts into bulklike crystalline benzene, the α_3 state, upon annealing or at coverages above 6 ML. These states are observed to desorb between 120 and 180 K. The growth mode of bulklike benzene is most likely in the form of 3-dimensional clusters as in the Stranski−Krastanov growth mode.[22] The crystalline benzene is always covered by a single amorphous layer as shown by infrared spectroscopy.[21] In this report one monolayer (ML) is defined as the number density of benzene molecules in the chemisorbed layer.

Laser-induced desorption of benzene multilayers has previously only been studied for micrometer-thick films with nanosecond lasers with either resonant infrared[23] or UV excitation.[24] In both cases the desorption/ablation of the benzene films is thermally induced.

In this paper, we contrast our previously measured coverage dependence[1] of femtosecond laser-induced desorption with 200 ps induced desorption. In addition, we recorded the fluence dependence at both pulse widths showing that translational energies of the desorbates increase with increasing fluence. We then bridged the gap between these two pulse widths by performing a pulse width variation at constant fluence, which shows a small but significant increase in yield and temperature of the prompt feature as the duration of the laser pulse is increased from 150 fs to 10 ps. These observations provide evidence for a process initiated by thermally assisted DIET excitation at the metal−benzene interface followed by efficient energy transfer across the multilayer.

II. Experimental Section

The Pt{111} crystal was mounted on a rotatable *xyz* translation stage contained in an ultrahigh vacuum chamber with a base pressure of 10^{-10} Torr. The crystal could be resistively heated to 1200 K and liquid nitrogen cooled to 100 K for these experiments. The chamber is equipped with a hemispherical electrostatic analyzer, electron gun, LEED optics, and sputter gun for surface analysis and cleaning. The crystal was cleaned by argon ion sputtering and oxidation/anneal cycles until there was no carbon detectable in an Auger spectrum and the oxygen desorption spectrum showed a well-developed recombinative desorption peak between 600 and 950 K.[25] Benzene is cleaned by several freeze−pump−thaw cycles until a residual gas spectrum taken in the UHV chamber displayed no impurities. Benzene was dosed at a crystal temperature of 110 K. After each laser desorption run, the residual benzene multilayer was desorbed by heating the crystal to 200 K, leaving the chemisorbed benzene layer on the surface. This dosing procedure avoided carbon contamination of the surface by thermal cracking of benzene.

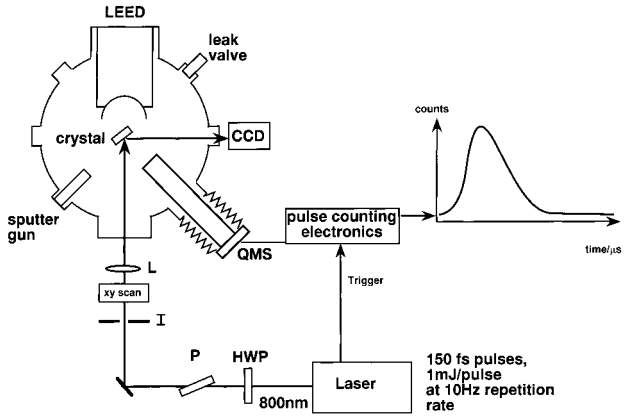

Figure 1. A schematic experimental setup of the surface analysis chamber and laser system employed in this investigation: HWP, half-wave plate; P, polarizer; I, iris; L, lens.

The laser source used in this work was an Ar^+-pumped Ti:sapphire oscillator (Spectra Physics Inc., Tsunami) regeneratively amplified at 10 Hz (Spectra Physics Inc., TSA 10). The regenerative amplifier was pumped by the second harmonic of a Nd:YAG laser (GCR-130). Pulses of between 150 fs and 200 ps duration at $\lambda = 800$ nm were employed, and the pulse width was measured routinely by an autocorrelator. Longer pulses are obtained by varying the amount of compression after regenerative amplification. 200 ps pulses are produced by bypassing the compressor stage completely.

Figure 1 depicts a schematic diagram of the optical arrangement used in this work. The beam diameter was controlled by a 3 mm diameter iris before the scanning unit that rastered the laser beam across the metal surface. The scanning unit could not be synchronized to the laser pulses but moved the laser spot on average 600 μm in the *x*-direction and 200 μm in the *y*-direction in a serpentine shape. Increasing the step size along *y* further did not change the form of spectra. The beam was directed onto the Pt{111} surface at 45° and focused to a 270 μm diameter spot, as calculated from the measured focal length of the lens and the measured distance to the crystal. For intensity-dependent measurements, the incident pulse energy was varied by a combination of half-wave plate and polarizer. Beam profile and pulse energy are measured with a CCD camera and an energy meter, respectively, after exiting the chamber. The laser fluence was then calculated from the measured pulse energy and the top-hat profile recorded by the CCD camera as scaled to the spot size on the crystal. While a given fluence is reproducible to better than 5%, the absolute value, due to uncertainty in the calculated spot size, lies within ±20% of the cited value.

A quadrupole mass spectrometer (QMS) was mounted along the surface normal to measure time-of-arrival distributions. The drift time of ions inside the QMS was determined by varying the QMS−crystal distance. Traces were acquired using a

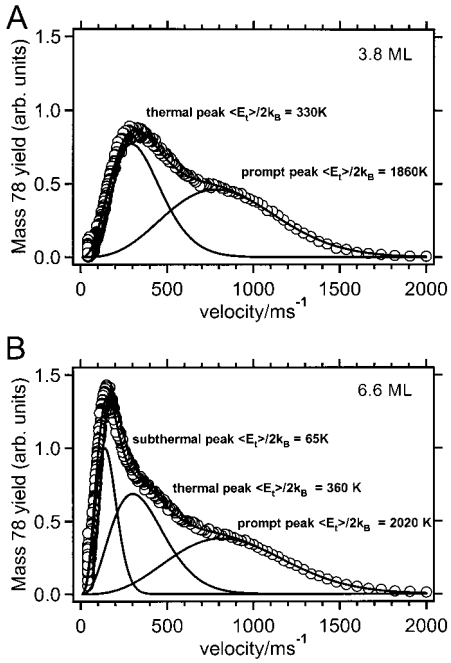

Figure 2. Velocity distributions for 150 fs duration laser desorption measured at benzene multilayer coverages of 3.8 and 6.6 ML.

multichannel scaler in 2 μs time bins for 8 ms with the QMS in pulse counting mode, and converted from time space to velocity space using the appropriate Jacobian.[26]

III. Results and Discussion

Coverage Dependence for 150 fs and 200 ps Induced Desorption. In our previous study of the coverage dependence of the 150 fs laser induced desorption of multilayer benzene,[1] we showed that the time-of-arrival distributions contain up to three peaks, which can be analyzed quantitatively by fitting them to a sum of the following modified Maxwell−Boltzmann distribution:

$$f(t) = \frac{a}{t^4}\exp\left(-\frac{m}{2k_B T}\left(\frac{d}{t} - u\right)^2\right) \qquad (1)$$

where a is a proportionality constant, t is time, d is the distance of flight, and u is a constant used to offset either for a stream velocity due to collisional processes in the gas phase or a residence time of the molecule on the surface before desorption. Molecules from the top of the benzene multilayer escape first and desorb in the fastest of the three peaks as shown by an experiment with layered films of isotopically labeled benzene.[1] Their velocities will therefore be hardly altered by collisions and we fit the fastest peak without a stream velocity. The other two peaks are typically wider than a Maxwell−Boltzmann distribution and their energy is calculated as a flux-weighted mean $\langle E_t \rangle$[27] to take account of the stream velocity. For convenience, we express the averaged translational energies as translational temperatures, where $\langle T_t \rangle = \langle E_t \rangle / 2k_B$. This does not imply that we are observing equilibrated ensembles.

As described previously, the distributions have to be fit with a minimum number of two Maxwellian distributions for coverages up to 6 ML (Figure 2A). The fits revealed a hyperthermal or prompt distribution that corresponds to a translational temperature of the order of 2000 K and a thermal distribution corresponding to a translational temperature of around 300 K. There can also be a subthermal peak corresponding to energies below 100 K for coverages above 6 ML (Figure 2B).

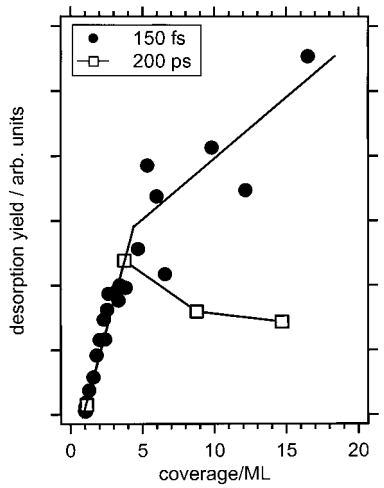

Figure 3. Coverage dependence of the total desorption yield for 150 fs pulses (filled circles) and for 200 ps laser pulses (open squares).

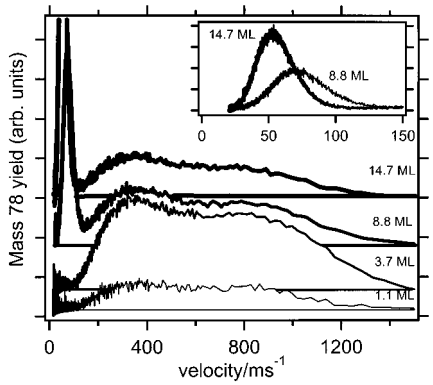

Figure 4. Velocity distributions for 200 ps induced desorption for benzene multilayer coverages between 1.1 and 14.7 ML. The inset shows an enlargement of the subthermal peak at 8.8 and 14.7 ML.

In our previous study we found that the desorption intensity of the prompt peak increases with coverage to a maximum at around 3−4 ML and then stays constant up to 20 ML. The translational energy of the prompt molecules was found to be constant within ±10%, the variation being correlated with the change in adsorption energy of the different benzene layers.

Not only does the intensity of the prompt peak show a change in slope between 3 and 4 ML but also the thermal intensity and consequently the total desorption yield as shown in Figure 3. This change in desorption cross section coincides with the beginning growth of crystalline benzene (α_3 peak in TPD) on top of the amorphous α_2 layer. The subthermal peak only becomes distinctly visible above 6 ML and coincides with the crystallization of the α_2 layer during exposure,[21] but since its peak maximum shifts strongly to lower velocities with increasing coverage it might be present at lower coverages but at first hidden by the thermal peak.

For 200 ps induced desorption, we find that the temperature of the prompt and thermal features does not change markedly with increasing multilayer thickness. The most probable velocity of the prompt feature ranges between 800 and 900 ms^{-1} for these coverages (Figure 4). The fact that the temperature of the prompt distribution remains constant as a function of film thickness for the 200 ps laser desorption again suggests that this feature is produced in the near-vacuum region as we have shown previously for 150 fs induced desorption. The total desorption yield (and the intensities of the prompt and thermal features), however, shows a different behavior (Figure 3). While

there is still an initial increase from 1.1 to 3.7 ML, the yield then drops by about 30% at higher coverages. Again, there is a coincidence of this decrease with the onset of bulk benzene growth.

The other striking difference from the previously taken spectra is that the subthermal peak appears at much lower velocities and is now quite separated from prompt and thermal peaks (Figure 4 in comparison to Figure 2B). Specifically, its translational temperature decreases from 13 K at 8.8 ML to 8 K at 14.7 ML and the distributions require a positive stream velocity for a good fit. In the case of 150 fs induced desorption the temperature decreased from 64 K at 6.6 ML to 34 K at 16.5 ML. The prominent subthermal feature is only observed at such low velocities when the long duration laser pulse is employed. This subthermal temperature is lower than the manipulator temperature and thus must have a nonthermal origin. One possible explanation for the subthermal distribution would be the formation of slow moving benzene clusters when high multilayer coverages are being desorbed. Taking the manipulator temperature of about 120 K as a reference, then for the 150 fs desorption the cluster size would be 2−4 molecules and for the 200 ps desorption it would lie in the range of 9−16 molecules. The benzene clusters would dissociate in the electron impact region of the mass spectrometer to give rise to the signal at $m/e^- = 78$ amu. Another explanation for the slow moving benzene distribution would be a desorption mechanism that involved a long surface residence time. This residence time would then have to increase with increasing multilayer coverage and increasing laser pulse width.

The laser intensity has changed by more than a factor 1000 between our previous and these measurements, and while there is a definite decrease in the desorption cross section of the prompt peak, it still shows qualitatively the same behavior, suggesting the same desorption mechanism.

Finally, it is remarkable that, even at our lowest coverage of 1 ML and for both pulse widths, there is always a prompt *and* a thermal distribution needed to fit the spectra and the ratio of their yields changes only slightly over the whole coverage range. So even when we desorb just from the chemisorbed layer with only one kind of adsorption state for the benzene molecule, a bimodal distribution is produced.

Fluence Dependence of the Desorption Process at 150 fs. The previous data suggest that not the laser intensity but rather the laser fluence might be the important parameter in the desorption process. To analyze the fluence dependence of the desorption process we first plot the total yield as a function of laser intensity for 3 ML coverage in Figure 5. Since benzene desorbs intact even at the highest fluence employed, we concentrated on measurements made at $m/e^- = 78$ amu for absorbed laser fluence between 26 and 200 mJ cm^{-2}. This corresponds to intensities between 7×10^{10} and 5.3×10^{11} W cm^{-2}. The plot reveals that there is an apparent threshold to desorption of approximately 30 mJ cm^{-2}, corresponding to 8×10^{10} W cm^{-2}. Calculation of the lattice temperature[28] shows that a maximum temperature of 1200 K is obtained for the Pt surface while an average temperature jump of 450 K is maintained for 100 ps. In the case of nanosecond heating of adsorbate−surface systems, a well-defined threshold for desorption is not usually observed because of the exponential dependence of the rate on temperature. Above the apparent threshold energy for desorption we measure a superlinear increase in the desorbate yield that can be fit to a third-order dependence of the laser intensity. A log−log plot of yield versus absorbed laser fluence reveals that the observed threshold is most likely due to our detection sensitivity.

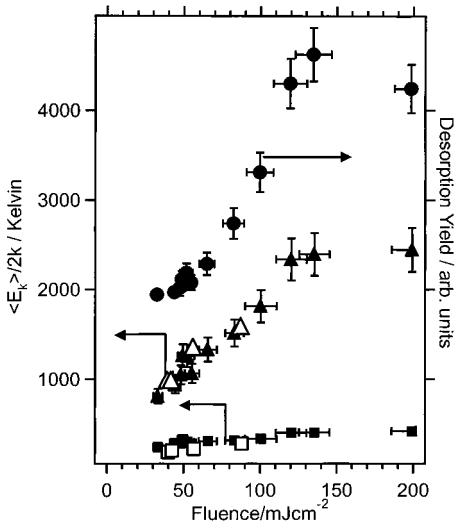

Figure 5. Fluence dependence of yield (filled circles) and translational temperature of prompt (filled triangles) and thermal (filled squares) peaks for 150 fs desorption. Open symbols are translational temperatures for 200 ps laser pulses.

Above approximately 120 mJ cm^{-2} the desorption yield saturates and this is attributed to complete desorption of the multilayer feature. Calculations reveal that the maximum lattice temperature obtained is 3600 K with an average of 1100 K over 100 ps. The saturation intensity was observed to increase with increasing coverage in the benzene multilayer. In the case of a 6 ML experiment there is no plateau in the yield at the highest intensities available for these experiments. This suggests that the maximum laser intensity available was insufficient to remove the entire multilayer.

The temperatures fit to the velocity distributions are plotted as a function of laser intensity in Figure 5. As can be seen, there is a linear dependence of the translational temperature on the laser fluence up to 120 mJ cm^{-2} for both prompt and thermal features. The translational temperature of the prompt peak at our detection threshold is 800 K. This is greater than the average temperature of 450 K of the Pt lattice calculated over the first 100 ps and less than the calculated peak temperature of 1200 K. The observation that the temperature of the prompt feature is not in equilibrium with the surface temperature is in accordance with the hypothesis that the prompt feature originates in the outermost layers of the multilayer structure.[1] In the case of the thermal peak, the temperature of the distribution increases linearly from 275 K at threshold to 400 K at 200 mJ cm^{-2} fluence. This trend and the kinetic energies are consistent with a thermal heating mechanism.

The prompt feature displays a maximum in kinetic energy at approximately 120 mJ cm^{-2} fluence. This maximum corresponds to the plateau in desorption yield. One might conclude that the correspondence indicates an importance of collisional processes in the gas phase for producing high kinetic energy species. In this scenario, desorption of additional molecules into the gas phase would produce more collisions in the adiabatic expansion and thus a higher terminal stream velocity.[4] However, in our coverage-dependent measurements the total yield changes by a factor 20 while the translational energies stay constant within 10%. This is not consistent with the major component of kinetic energy coming from gas phase adiabatic expansion. Also, as the translational temperature of the prompt feature

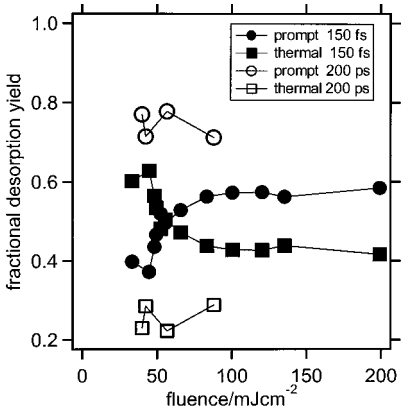

Figure 6. Fractional desorption yield of prompt and thermal distributions for 150 fs (filled symbols) and 200 ps (open symbols) induced desorption.

increases, there is no apparent stream velocity as would be expected for collisional cooling.

Alternatively, the plateau in the kinetic energy distribution as a function of laser fluence may indicate the presence of a different desorption mechanism with a threshold near 120 mJ cm^{-2}. Such a mechanism might be a direct desorption mechanism of the benzene where a three-photon absorption becomes probable at the intensity of 3.2×10^{11} W cm^{-2}. However, as shown below, the temperature of the prompt feature depends on fluence rather than intensity, making a multiphoton mechanism more unlikely.

The plateau most likely corresponds to a limit in the amount of energy that can be transferred from the Pt surface into the film before desorption occurs. In this case the final translational temperature of the benzene is the product of the amount of energy deposited into the Pt and the probability of further transfer into the benzene layer. The energy deposited into the metal lattice depends only on the number of incident photons. The amount of energy transferred into the benzene depends both on the Pt energy and the residence time of the multilayer on the surface.

The measured desorbate distribution can be deconvolved into prompt and thermal components as shown by the filled symbols in Figure 6 as fractions of the total desorption yield as a function of fluence. There is a definite change around 50 mJ cm^{-2}. At low fluence, there are relatively fewer molecules desorbing in the prompt peak than at higher fluence.

Fluence Dependence at 200 ps. For comparison, velocity distribution measurements were made as a function of fluence at 200 ps pulse width. The desorbate velocity distribution as a function of fluence of the 200 ps duration laser pulse at a coverage of 4 ML was measured over the range 20−90 mJ cm^{-2} only, to avoid laser-induced damage, which becomes more likely when the surface is heated above 1000 K with nanosecond duration laser pulses.[29] The resulting translational temperatures, as shown by the open symbols in Figure 5, are the same as for 150 fs desorption. The total desorption yield also increases with increasing fluence, similarly to the 150 fs case. The coverage dependence of the fractional yields of prompt and thermal peaks is very different, though, from the femtosecond case (Figure 6): the contribution of each peak is now *independent* of fluence above our observation threshold.

Pulse Duration Dependence of the Desorption Process. Having established that 150 fs and 200 ps duration pulses result in qualitatively similar kinetic energy distributions, we finally investigated what the quantitative change in going from femtosecond to picosecond induced desorption is.

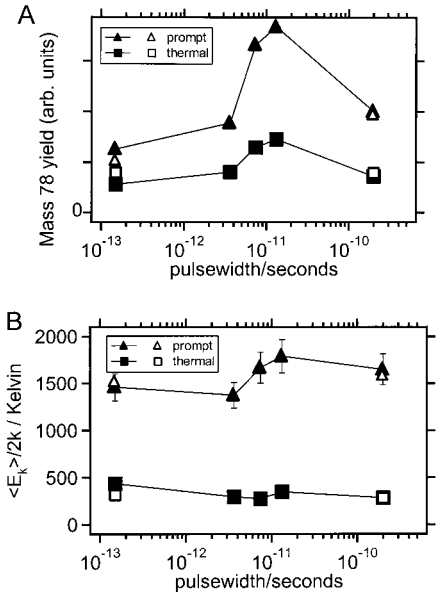

Figure 7. Pulse width dependence of partial desorption yields (A) and translational temperatures (B) of prompt and thermal distribution at 80 mJ cm^{-2}. Open symbols show the corresponding data points from Figures 5 and 6.

To probe the velocity distribution of laser desorbed benzene as a function of pulse duration, measurements were performed at constant laser fluence (80 mJ cm^{-2}) while the laser pulse duration was increased from 150 fs to 200 ps. The yield of the prompt and thermal features is plotted as a function of pulse duration in Figure 7A for the case of 4 ML of benzene. The thermal yield doubles and the prompt yield triples as the pulse duration is increased from 150 fs to 13 ps. Above 13 ps, the intensity of each feature decreases by approximately a factor of 2. The latter measurement was made with the uncompressed pulse of approximately 200 ps pulse duration. We conclude that less energy is coupled into the multilayer when the longest duration laser pulse is employed. This may be because the mechanism of desorption is changing or because the time scale for desorption is beginning to compete with the time scale for transferring energy from the hot Pt lattice to the benzene multilayer.

The translational temperatures resulting from the modified Maxwellian fits to the velocity distributions are plotted in Figure 7B for the prompt and thermal features as a function of laser pulse duration. The translational temperature of the thermal feature decreases only slightly from 450 to 400 K as the pulse duration is increased from 150 fs to 200 ps. In the region of the large increase in desorption yield for 13 ps pulse duration there is essentially no evidence for a corresponding increase in translational temperature. This can be contrasted with measurements made as a function of laser fluence where increasing desorption yield correlated with increasing translational temperature of the thermal feature. We conclude from this that postdesorption collisions are not necessarily responsible for the increase in translational temperature observed in the fluence and previous coverage-dependent measurements.[1] The translational temperature of the prompt feature increases by approximately 30% from 1450 to 1750 K upon increasing the pulse duration from 150 fs to 13 ps. In this case there is a positive correlation with the desorption yield. This trend is consistent with the hypothesis that the prompt feature is not created by the same mechanism that produces the thermal feature.

At this point it is helpful to summarize our findings. We have varied the intensity of the incident laser pulse in two ways. In

the first case, we kept the pulse width constant and found that an increase in fluence is accompanied by an increase in desorption yield and an increase in translational energy of the desorbing molecules. In the second case, we kept the fluence constant and found that an increase in pulse width up to 13 ps (i.e., a decrease in intensity) is accompanied by, again, increasing yield and increasing translational energy for the prompt feature, though decreasing translational energy for the thermal feature. This shows that, for the prompt desorption feature, the fluence rather than the intensity is the determining factor in the desorption mechanism.

Possible Desorption Mechanisms. The trends observed in the case of the 200 ps laser desorption experiments are similar to those observed in the case of 150 fs duration desorption. This suggests that the mechanism of desorption is similar for laser pulse duration spanning 3 orders of magnitude and is therefore essentially driven by the number of absorbed photons and not the time scale of their arrival. This places severe restrictions on potential mechanisms of desorption.

To begin with, we will briefly discuss standard models that have been invoked for laser-induced desorption, before introducing a new model to explain the observed phenomena.

Thermal Models. Typical for laser-induced thermal desorption (LITD) at high heating rates are the following characteristics: a threshold for significant desorption yields, a nonlinear increase of yield with fluence, and a linear translational energy dependence on fluence. So our observed phenomena are strongly reminiscent of LITD with one important exception. A thermal model alone cannot explain why, even for coverages as low as 1 ML with only one benzene adsorption state, a bimodal time-of-arrival distribution should be observed.

Electronic Models. A nonlinear increase in yield and a linear dependence of the translational energy on fluence have also been found in DIMET of O_2/Pt{111}[30] and CO/Cu{100}.[31] The main drawback of this scheme is that the efficiency of the DIMET process is intensity dependent. As the pulses are broadened into the sub-nanosecond regime one would expect the character of desorption to change to DIET-like behavior (as observed for O_2/Pt{111}[32]). This would become apparent as a translational energy of the molecules which is independent of fluence, contrary to what we observe.

At the high laser intensities we use, it is possible that photoelectrons are emitted from the surface. If their yield is high enough a space charge should build up, driving photoelectrons back to the surface where they could conceivably initiate desorption. But since our photon energy is only 1.55 eV and the work function of 1 ML benzene on a platinum surface is 4.4 eV,[33] photoelectrons can only be emitted via multiphoton excitation. This effect should therefore be strongly intensity dependent and thus would "switch off" for longer duration pulses.

Another possible mechanism would be the *optical* excitation of the physisorbed benzene molecule into a long-lived vibronic state. Such a state exists at a transition (6_1^0) of 266.67 nm, exactly 3 times the energy of the 800 nm photon, so that the third-order dependence of the yield on fluence could be explained by a three-photon excitation of the benzene molecule. This state has a lifetime of 100 ns in the gas phase.[34] Even if the lifetime was reduced in the condensed phase, it could conceivably still be long enough to make little difference whether this state is excited with femtosecond or sub-nanosecond pulses, as has been shown in gas phase multiphoton ionization experiments.[35] To test this hypothesis we varied the wavelength between 790 and 830 nm. We found no change in the time-of-arrival spectra and therefore exclude this excitation mechanism.

Since neither phonon- nor electron-based mechanisms alone can explain the full range of benzene desorption phenomena, we propose a new hybrid model, described below.

Vibrationally Assisted DIET and Newton's Cradle. Since neither standard phonon- nor electron-based mechanisms alone can explain the full range of benzene desorption phenomena in the monolayer and multilayer regimes, we propose a new model. This invokes vibrationally assisted electronic excitation in the chemisorbed layer to *initiate* the desorption process, followed by a phonon transfer mechanism ("Newton's cradle") for the efficient transport of energy to the outer layers at higher multilayer coverages.

A. Vibrationally Assisted Electronic Excitation in the Chemisorbed Layer. If photon-induced electronic excitation of chemisorbed (first layer) benzene is to be invoked in the initiation step of the desorption process, we need to ascertain the lowest unoccupied state of the mixed-orbital states of benzene plus Pt metal. Calculations[36] of the STM image of an isolated benzene molecule on Pt{111}[37] using a molecular orbital approach as well as cluster calculations[38] place the antibonding states in the range 2−3 eV above the Fermi level. Inverse photoemission of benzene on Rh{111}[39] and NEXAFS of benzene on Cu{110} and Ni{100}[40] confirm these calculations. Moreover, in a recent density functional theory, gradient density corrected, slab calculation of benzene on Ni{111} in a $(\sqrt{7}\times\sqrt{7})R19.1°$ structure,[41] which closely reproduces the results of a detailed LEED structural study,[42] the antibonding states are again found at between 2 and 3 eV above E_F. Since the photon energy in the present study is 1.55 eV, we conclude that photoelectron excitation alone is insufficient to populate the lowest antibonding states of the benzene−Pt system. Instead, we propose, as outlined below, that the Franck−Condon excitation to the electronically excited state takes place from a vibrationally excited state of the ground electronic state, where the excitation energy to the unstable state is 1.55 eV. Once in the electronically excited state, the molecule can begin to move away from the metal surface, gaining kinetic energy as it moves on the repulsive potential of the upper state.

A laser pulse penetrates the benzene multilayer without attenuation, as there are no excitations of solid benzene around 1.55 eV. As the pulse reaches the metal−benzene interface, photons are strongly absorbed in the metal surface region by electron−hole pair excitations, the electronic temperature being raised in this region on the time scale of the laser pulse duration. The lattice temperature of the combined metal−surface layer plus chemisorbed layer system rises on a longer time scale, in the region of a few picoseconds,[43] which is determined by the electron−phonon coupling strength. However, even on the time scale of the shortest pulses used in the present work, 150 fs, phonon excitation will have significantly populated higher vibrational states of several lower frequency modes of the benzene−metal system. After initiating vibrational excitation with the initial portion of the laser pulse envelope, the remainder of the laser pulse may induce transfer to the benzene−metal excited state by a Franck−Condon excitation, as depicted in Figure 8, with an excitation energy in the region of the incident photon energy. This can be achieved by direct photoelectron excitation or via hot electrons. In this way, photons in the first part of the laser pulse will lead, via phonon excitation of the substrate, to vibrational ladder climbing of the ground state molecules, while photons in the second part of the laser pulse

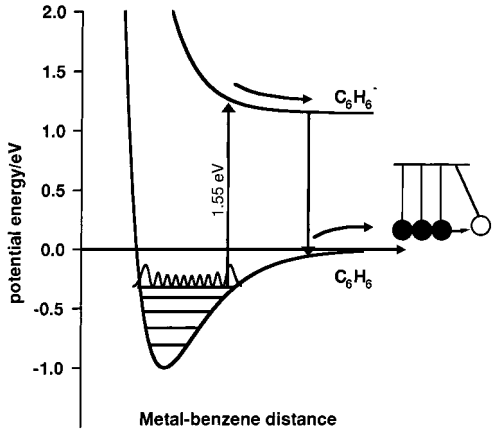

Figure 8. A schematic of a thermally-assisted DIET process. The chemisorption energy of benzene is approximately 1 eV. The excited state shown is the anionic state of benzene with a gas phase electron affinity of 1.15 eV. As shown, this excited state can be accessed with 1.55 eV photon energy from an upper vibrational level. The impulse from the chemisorbed layer can be transferred to the upper benzene layers via a molecular Newton's cradle as sketched on the right-hand side of the figure.

will cause electronic excitation to antibonding states. The molecules can then gain enough kinetic energy on the excited PES to finally desorb from the ground state PES with an excess energy of about 0.07 eV or 800 K (compare Figure 5) at the observed threshold of desorption, unless this energy is transferred by collision with other benzene molecules in the multilayer prior to desorption.

The mechanism schematically illustrated in Figure 8 shows, for simplicity, electronic excitation from the $\nu = 10$ vibrational state, matched by a 1.55 eV excitation energy to the antibonding excited state PES. The benzene−platinum stretch mode has been observed at 360 cm^{-1} (45 meV).[44] Assuming a Morse potential[48] then at a surface temperature of 1000 K, vibrational states $\nu =$ 10 or higher have a total population of 1%. Vibrational excitation of other modes, such as the ring-breathing modes of the carbon skeleton or the out-of-plane CH wagging modes, may also be involved, but here we note that excitation of the molecule−surface mode along the desorption coordinate reduces the threshold energy for a Franck−Condon transition in two ways: one by vibrational ladder climbing and the other by the lowering of the total energy of the excited state molecule−surface system along the same coordinate.

The initiation of the desorption process by thermally-assisted DIET, as described above, is uniquely consistent (among all the models we have examined) with the pulse width dependence of desorption process shown in Figure 7A. If the laser pulse is very short (150 fs), population of the higher molecule−surface vibrational states will be too low for efficient electronic excitation while the pulse is still on. However, as the pulse is lengthened, the higher vibrational levels become well populated while the laser is on, so that the electronic excitation becomes more efficient. Our measurements show the optimal pulse width to be around 10−20 ps. At even longer pulse widths, the efficiency of the process decreases because the maximum achievable lattice temperature, and therefore the degree of vibrational preheating, is now much lower.

In further support of this model for the initiation process, we note that there is experimental evidence from semiconductor and insulator surfaces[45,46] and theoretical evidence for NO/Pt{111}[47] that an increase in surface temperature can increase the DIET (or DIMET) desorption yield by a factor 2−4. With pulsed laser heating and very high transient temperatures, much higher vibrational levels should be accessed.

The monotonic dependence of the prompt yield, and translational energy, on fluence (Figure 5) is also fully consistent with this initiation mechanism. As the fluence is increased at constant pulse width, the maximum electronic and lattice temperatures of the system are increased in a near-linear fashion, and so efficient vibrational heating is achieved earlier during the laser pulse before the DIET process sets in. The increasing efficiency of prompt desorption with increasing fluence for 150 fs desorption is shown in Figure 6. We noted before that at the lowest fluence the spectra could be fitted with a single broadened translational energy distribution, corresponding to thermally induced desorption. It is the prompt desorption peak that is directly associated with the vibrationally assisted electronic excitation mechanism, and the cross section for this process is low at low fluences.

For thick benzene layers only a small fraction of molecules undergo this process, but since they desorb translationally hot their angular distribution is strongly forward peaked thus leading to a higher detection rate in the QMS. The rest of the molecules desorb in the thermal peak (laser-induced thermal desorption). This peak is broadened because of the large number of molecules desorbed in one shot. This leads to gas phase collisions above the surface, a full range Maxwellian develops and some molecules will move back toward the surface. They will stay there for a certain residence time, depending on the temperature of the surface at that time, and the redesorb again, adding to the time-of-arrival signal at later times. The broadening is less pronounced at lower coverages, as would be expected from this scenario.

B. Propagation of Kinetic Energy across the Multilayer. As shown experimentally with isotopomers,[1] the benzene molecules desorbing from a multilayer into the prompt desorption peak originate from the outermost benzene layers. In our model, the impulse for this process is nevertheless generated, as described above, in the first, chemisorbed layer. This impulse takes the form of an excited state, or ground state, benzene molecule moving with a translational energy of $\geq$0.07 eV away from the metal surface. Clearly, energy transfer will take place with benzene molecules in successive layers, each intervening layer experiencing a recoil from the layer above it. The last layer, at the benzene−vacuum interface, will desorb into the vacuum if the energy transferred to it exceeds the benzene condensation energy.

In this way, the energy is transferred by a soliton phonon wave (in the ideal case) from the chemisorbed layer, where the initiation process (Figure 8) occurs, to the outermost layer. This process can be described as a molecular Newton's cradle, shown as an inset to Figure 8.

This second stage of the desorption mechanism is also fully consistent with experimental observation. We have found the following.

1. For multilayer coverages there is little variation in translational energy of the prompt peak with layer thickness.[1]

2. The cross section for desorption in the prompt peak is initially constant—up to about 3−4 ML the partial prompt desorption yield increases linearly with coverage. At higher coverages the yield then reaches a plateau. This coincides with the onset of bulk benzene growth. With 3D islands being formed the film will reach its maximum surface area around 4 ML and our model for a Newton's-cradle-like energy transfer requires that the finally desorbing molecules can escape without further collisions.

3. When the coverage is increased beyond 6.5 ML, the density of the thermally desorbing gas is sufficiently high for benzene clusters to form. Molecular density and velocity in the plume will determine the average cluster size and the latter will therefore be a complex function of laser pulse width.

In conclusion, we have shown that a hybrid model in which kinetic energy is generated in the first chemisorbed layer by a DIET mechanism, assisted by vibrational preheating, and followed by a molecular Newton's cradle for energy transfer from the bottom to the top of the benzene film, can qualitatively explain the large range of phenomena displayed by laser-induced desorption of benzene mono- and multilayers. We are currently developing a theoretical model to explain our data in more detail, which will be discussed in a forthcoming paper.[48]

Acknowledgment. H.A. and C.R. acknowledge TMR grants by the European Union, R.J.L. acknowledges the support of the National Science Foundation through a Young Investigator Award and CHE9976476. The support of EPSRC, the Isaac Newton Trust and the Royal Society of Chemistry for equipment and the Sloan and Dreyfus Foundations is also greatly appreciated.

References and Notes

(1) Arnolds, H.; Rehbein, C. E. M.; Roberts, G.; Levis, R. J.; King, D. A. *Chem. Phys. Lett.* **1999**, *314*, 389.
(2) Karas, M.; Bachmann, D.; Bahr, U.; Hillenkamp, F. *Int. J. Mass Spectrom. Ion. Processes* **1987**, *78*, 53.
(3) Ellegaard, O.; Schou, J. *J. Appl. Phys.* **1998**, *83*, 1078.
(4) NoorBatcha, I.; Lucchese, R. R.; Zeiri, Y. *Surf. Sci.* **1988**, *200*, 113.
(5) Papageorgopoulos, D. C.; Ge, Q.; Nimmo, S.; King, D. A. *J. Phys. Chem B* **1997**, *10*, 1999.
(6) Levine, R. D.; Bernstein, R. B. *Molecular Reaction Dynamics and Chemical Reactivity*; Oxford University Press: New York, 1987.
(7) Zhu, X.-Y. Annu. *Rev. Phys. Chem.* **1994**, *45*, 113.
(8) Zimmermann, F. M.; Ho, W. *J. Chem. Phys.* **1994**, *100*, 7700.
(9) Buntin, S. A.; Richter, L. J.; King, D. S.; Cavanagh, R. R. *J. Chem. Phys.* **1989**, *91*, 6429.
(10) Prybyla, J. A.; Heinz, T. F.;Misewich, J. A.; Loy, M. M. T.; Glownia, J. H. *Phys. Rev. Lett.* **1990**, *64*, 1537. Misewich, J. A.; Heinz, T. F.; Newns, D. M. *Phys. Rev. Lett.* **1992**, *68*, 3737.
(11) Ho, W. *Surf. Sci.* **1996**, *363*, 166.
(12) Beavis, R. C.; Chait, B. T. In *Methods and Mechanisms for Producing Ions from Large Molecules*; Standing, K. G., Ens, W., Eds.; Plenum Press: New York, 1991; p 227.
(13) Zhou, J.; Ens, W.; Standing, K. G.; Verentchikov, A. *Rapid Commun. Mass Spectrom.* **1992**, *6*, 671.
(14) Menzel, D.; Gomer, R.; *J. Chem. Phys.* **1964**, *41*, 3311. Redhead, P. A. *Can. J. Phys.* **1964**, *42*, 886.
(15) Hall, R. B.; De Santolo, A. M. *Surf. Sci.* **1984**, *137*, 421.
(16) Fann, W. S.; Storz, R.; Tom, H. W. K.; Bokor, J. *Phys. Rev. B* **1992**, *46*, 13592; Elsayed-Ali, H. E.; Norris, T. B.; Pessot, M. A.; Mourou, G. A. *Phys. Rev. Lett.* **1987**, *58* 1212.
(17) Mann, S. S.; Todd, B. T.; Stuckless, J. T.; Seto, T.; King, D. A. *Chem. Phys. Lett.* **1991**, *183*, 529.
(18) Campbell, J. M.; Seimanides, S.; Campbell, C. T. *J. Phys. Chem.* **1989**, *93*, 815.
(19) Lehwald, S.; Ibach, H.; Demuth, J. E. *Surf. Sci.* **1978**, *78*, 577.
(20) Tsai, M. C.; Muetterties, E. L. *J. Am. Chem. Soc.* **1982**, *104*, 2534.
(21) Jakob, P.; Menzel, D. *J. Chem. Phys.* **1996**, *105*, 3838.
(22) Jakob, P.; Menzel, D. *Surf. Sci.* **1989**, *220*, 70.
(23) Braun, R.; Hess, P. *J. Chem. Phys.* **1993**, *99*, 8330.
(24) Georgiou, S.; Koubenakis, A.; Kontoleta, P.; Syrrou, M. *Laser Chem.* **1997**, *17*, 73.
(25) Steininger, H.; Lehwald, S.; Ibach, H. *Surf. Sci.* **1982**, *123*, 1.
(26) Auerbach, D. J. In *Atomic and Molecular Beam Methods*; Scoles, G., Ed.; Oxford University Press: London, 1988; Vol. 1.
(27) $\langle E_t \rangle = \int dt\, f(t) t^{-1} E_t / \int dt\, f(t) t^{-1}$ reduces to $2k_B T_t$ for $u = 0$.
(28) Anisimov, S. I.; Kapeliovich, B. L.; Perel'man, T. L. *Zh. Eksp. Teor. Fiz.* **1974**, *66*, 776 (*Sov. Phys. JETP* **1974**, *39*, 375).
(29) Frohn, J.; Reynolds, J.; Engel, T. *Surf. Sci.* **1994**, *320*, 93.
(30) Busch, D. G.; Gao, S.; Pelak, R. A.; Booth, M. F.; Ho, W. *Phys. Rev. Lett.* **1995**, *75*, 673.
(31) Struck, L. M.; Richter, L. J.; Buntin, S. A.; Cavanagh, R. R.; Stephenson, J. C. *Phys. Rev. Lett.* **1996**, *77*, 4576.
(32) Busch, D. G.; Ho, W. *Phys. Rev. Lett.* **1996**, *77*, 1338.
(33) Dippel, O.; Cemic, F.; Hasselbrink, E. *Surf. Sci.* **1996**, *357*−*358*, 190.
(34) Spears, K. G.; Rice, S. A. *J. Chem. Phys.* **1971**, *55*, 5561.
(35) Weinkauf, R.; Aicher, P.; Wesley, G.; Grotemeyer, J.; Schlag, E. W. *J. Phys. Chem.* **1994**, *98*, 8381.
(36) Sautet, P.; Bocquet, M.-L. *Phys. Rev. B* **1996**, *53*, 4910.
(37) Weiss, P. S.; Eigler, D. M. *Phys. Rev. Lett.* **1993**, *71*, 3139.
(38) Anderson, A. B.; McDevitt, M. R.; Urbach, F. L. *Surf. Sci.* **1984**, *146*, 80.
(39) Netzer, F. P.; Frank, K.-K. *Phys. Rev. B* **1989**, *40*, 5223.
(40) Nilsson, A.; Wassdahl, N.; Weinelt, M.; Karis, O.; Wiell, T.; Bennich, P.; Hasselström, J.; Föhlisch, A.; Stöhr, J. *Appl. Phys. A* **1997**, *65*, 147.
(41) Yamagishi, S.; Jenkins, S.; King, D. A., to be published.
(42) Held, G.; Bessent, M. P.; Titmuss, S.; King, D. A. *J. Chem. Phys.* **1996**, *105*, 11312.
(43) Germer, T. A.; Stephenson, J. C.; Heilweil, E. J.; Cavanagh, R. R. *J. Chem. Phys.* **1993**, *98*, 9986. Struck, L. M.; Richter, L. J.; Buntin, S. A.; Cavanagh, R. R.; Stephenson, J. C. *Phys. Rev. Lett.* **1996**, *77*, 4576.
(44) Mate, C. M.; Somorjai, G. M. *Surf. Sci.* **1985**, *160*, 542.
(45) Xin, Q.-S.; Zhu, X.-Y. *Chem. Phys. Lett.* **1997**, *265*, 259.
(46) Thiel, S.; Klüner, T.; Wilde, M.; Al-Shamery, K.; Freund, H.-J. *Chem. Phys.* **1998**, *228*, 185.
(47) Saalfrank, P.; Kosloff, R. *Chem. Phys.* **1996**, *105*, 2441.
(48) Arnolds, H.; Levis, R. J.; King, D. A., to be published.